Asian Journal of Urology 10 (2023) 81–88

Available online at www.sciencedirect.com

ScienceDirect

journal homepage: www.elsevier.com/locate/ajur

Original Article

Validation of user-friendly models predicting extracapsular extension in prostate cancer patients

Leandro Blas, Masaki Shiota*, Shohei Nagakawa, Shigehiro Tsukahara, Takashi Matsumoto, Ken Lee, Keisuke Monji, Eiji Kashiwagi, Junichi Inokuchi, Masatoshi Eto

Department of Urology, Graduate School of Medical Sciences, Kyushu University, Fukuoka, Japan

Received 15 November 2021; received in revised form 16 December 2021; accepted 7 February 2022
Available online 22 April 2022

KEYWORDS
Prognosis;
Prostate cancer;
Nomogram;
Extracapsular extension

Abstract *Objective:* There are many models to predict extracapsular extension (ECE) in patients with prostate cancer. We aimed to externally validate several models in a Japanese cohort.
Methods: We included patients treated with robotic-assisted radical prostatectomy for prostate cancer. The risk of ECE was calculated for each patient in several models (prostate side-specific and non-side-specific). Model performance was assessed by calculating the receiver operating curve and the area under the curve (AUC), calibration plots, and decision curve analyses.
Results: We identified ECE in 117 (32.9%) of the 356 prostate lobes included. Patients with ECE had a statistically significant higher prostate-specific antigen level, percentage of positive digital rectal examination, percentage of hypoechoic nodes, percentage of magnetic resonance imaging nodes or ECE suggestion, percentage of biopsy positive cores, International Society of Urological Pathology grade group, and percentage of core involvement. Among the side-specific models, the Soeterik, Patel, Sayyid, Martini, and Steuber models presented AUC of 0.81, 0.78, 0.77, 0.75, and 0.73, respectively. Among the non-side-specific models, the memorial Sloan Kettering Cancer Center web calculator, the Roach formula, the Partin tables of 2016, 2013, and 2007 presented AUC of 0.74, 0.72, 0.64, 0.61, and 0.60, respectively. However, the 95% confidence interval for most of these models overlapped. The side-specific models presented adequate calibration. In the decision curve analyses, most models showed net benefit, but it overlapped among them.
Conclusion: Models predicting ECE were externally validated in Japanese men. The side-specific models predicted better than the non-side-specific models. The Soeterik and Patel models were the most accurate performing models.

* Corresponding author.
E-mail address: shiota.masaki.101@m.kyushu-u.ac.jp (M. Shiota).
Peer review under responsibility of Tongji University.

https://doi.org/10.1016/j.ajur.2022.02.008

1. Introduction

Surgical treatment for prostate cancer aims to achieve the "pentafecta" that includes preservation of potency and continence, negative surgical margins, no surgical complications, and freedom from biochemical recurrence [1]. Performing a nerve-sparing radical prostatectomy (NSRP) is fundamental to conserve potency and continence [2]. However, NSRP increases the risk of a positive surgical margin which has prognosis implications and increases the associated cost [3,4]. Thus, there is a delicate balance between the amount of tissue resected and the risk of a positive surgical margin.

Extracapsular extension (ECE) is defined as the continuation of the tumor beyond the confines of the prostate, independently from seminal vesicle involvement [5]. ECE was found in about 20% of specimens in men with clinically localized prostate cancer [6]. It is an independent adverse prognostic factor and is associated with a worse prognosis [6,7]. Imaging technologies such as computed tomography scan and magnetic resonance imaging (MRI) may help in ECE detection in low-risk prostate cancer patients and may aid in decision-making in NSRP, but present a limited performance due to low sensitivity for detecting T3a stage [8—10]. Therefore, a correct prediction of whether there is ECE or not, is a cornerstone to proper management of the disease, determining patients' eligibility and limiting the resection of tissue during NSRP [11,12].

However, the adequate way to choose candidates who benefit the most from NSRP has not been well elucidated. For this purpose, several tools (nomograms, linear simple formulas, and web calculators) that predict the probability of ECE have been developed and validated [13—21]. Some of these tools have been periodically updated incorporating new clinical data and insights regarding the procedure. Some of these models are available on a website and friendly to users, and patients can easily consult them.

Current American Urological Association guidelines recommend performing NSRP in patients with localized disease [22]. The European Association of Urology-European Society for Radiotherapy & Oncology-International Society of Geriatric Oncology guidelines for prostate cancer recommend not to preserve the neuro vascular bundle in patients with clinical stage higher than T2c, and with any biopsy International Society of Urological Pathology (ISUP) grade group higher than 3 and recommend to offer NSRP to patients with a low-risk extracapsular disease [7]. The National Comprehensive Cancer Network guidelines and the Japanese Urological Association guidelines do not stand a recommendation on the use of models to estimate the risk of ECE and select patients considered for NSRP [7,9,23].

However, most models for predicting ECE have not been externally validated at all or in Japanese. Given these facts, we aimed to externally validate models for predicting ECE in a Japanese cohort.

2. Patients and method

2.1. Patients and operation

The study has been approved by the institutional research ethics committee (approval number 2021—123, date 12/06/2021) and has been conducted in accordance with principles of the Helsinki Declaration. All patients gave their informed consents for participation in this research study.

We included a cohort of Japanese patients who underwent robot-assisted radical prostatectomy (RARP) between June 2009 and March 2021 at Kyushu University Hospital (Fukuoka, Japan) [24]. We included patients with diagnosis of carcinoma of the prostate that had complete clinical and histopathological results available and had a preoperative prostate MRI. We excluded patients with neoadjuvant treatment. Clinical and pathological data were collected prospectively in an electronic database. Individual patient data were used to calculate the risk of ECE in each nomogram. Tumor-node-metastases classification was used to assess clinical T-stage. ECE was defined as the continuation of the tumor beyond the confines of the prostate into the periprostatic tissue, independently from seminal vesicle involvement or bladder neck involvement [5]. RARP was performed by seven surgeons using the daVinci Surgical System (S, Si, and Xi, Intuitive Surgical, Sunnyvale, CA, USA). Neurovascular bundle preservation was performed combining anterograde and retrograde approaches and using a thermal technique. Patients were selected according to the operation date and the risk of ECE was determined by preoperative cancer risk, and preoperative patients' potency and preference [25,26].

2.2. Models predicting ECE

In all, 10 models and the Roach formula were validated [27]. All of them were available online and friendly to users. The Patel model (available in https://prece.it/) and the Memorial Sloan Kettering Cancer Center (MSKCC) web calculator (https://www.mskcc.org/nomograms/prostate/pre_op) were calculated using the website calculator. We also included the logistic regression models that are available on https://www.evidencio.com/home. This online platform allows researchers to translate prediction models into online calculators for application and external validation. The estimated prognostic of ECE was calculated for each patient. The variables included were preoperative prostate-specific antigen (PSA) level, PSA density, clinical T-stage obtained by digital rectal

examination, total Gleason score, the total number of cores, the number of positive and negative cores, and MRI or transrectal ultrasound findings, depending on each model. Side-specific models included the two prostate lobes, and the non-side-specific models included an overall calculation for each prostate gland.

2.3. Statistical analysis

Baseline characteristics were expressed as the median and interquartile range (IQR), or number and percentage. Comparisons between groups were performed using the Mann-Whitney, and Chi-square tests. Model performance was assessed by the area under the curve (AUC), calibration plots, and decision curve analyses. A logistic regression model was performed for each tool and the AUC was calculated to quantify model accuracy. AUC ranged between 0.5 and 1; AUC of 0.5 indicated no discrimination; $0.5<AUC<0.7$ indicated poor discrimination; $0.7\leq AUC<0.8$ indicated acceptable discrimination; $0.8\leq AUC<0.9$ indicated excellent discrimination; $0.9\leq AUC<1$ indicated outstanding discrimination; and AUC of 1 indicated perfect discrimination [28]. Logistic regression statistics were used to evaluate model estimation by performing calibration plots that showed the agreement between predicted and observed ECE. Calibration was assessed by calculating the calibration slope and intercept. When the former was close to 1 and the latter was close to 0, it indicated a good calibration among the range of individuals. The predicted risks were divided into deciles and a line obtained by locally weighted scatterplot smoothing was superimposed. A well-calibrated model showed predictions that lay at or around the reference line in the calibration plot. Model performance was assessed by AUCs, calibration plots, and decision curve analyses. Decision curve analyses were performed to show the net benefit of the models as a function of the threshold probability. The net benefit was to correctly identify which patients had ECE or not. The unit of net benefit was the ratio of true positives to the target population [29]. All statistical analyses were performed using Stata v.14 (College Station, TX, USA). The $p<0.05$ was considered statistically significant.

3. Results

Overall, after excluding by criteria 178 patients were included in this analysis. The median age was 66 (IQR 62–69) years and the median PSA was 8.2 (IQR 5.9–12.9) ng/mL. Only four (2.2%) patients presented bilateral ECE. The baseline characteristics of the cohort are shown in Table 1. Of the 356 prostate lobes included, 117 (32.9%) lobes had ECE in the histopathological analysis. The baseline characteristics of the cohort by prostate lobes are shown in Table 2. The median total biopsy cores by prostate lobe were 6 (IQR 5–6), and the median positive cores by prostate lobes were 2 (IQR 1–3). Most patients with ECE presented ISUP grade groups 3, 4, or 5 in the prostate biopsy, and only 10% presented ISUP grade group 1. On the other hand, a quarter of patients without ECE presented ISUP grade groups 3, 4, or 5. Patients with ECE had a statistically significant higher PSA level, percentage of positive digital rectal examination, percentage of hypoechoic nodes, percentage of MRI nodes or ECE suggestion, percentage of biopsy positive cores, ISUP grade group, and percentage of core involvement.

Table 1 Baseline patients' characteristics.

Characteristic	Value ($n=178$)
Age at surgery, median (IQR), year	66 (62–69)
PSA, median (IQR), ng/mL	8.2 (5.9–12.9)
PSA density, median (IQR), (ng/mL)/mL	0.29 (0.20–0.44)
Clinical stage, *n* (%)	
T1c	106 (59.6)
T2a	34 (19.1)
T2b	22 (12.4)
T2c	11 (6.2)
T3a	4 (2.2)
T3b	1 (0.6)
Pathological stage, *n* (%)	
T2	79 (44.4)
T3a	72 (40.4)
T3b	26 (14.6)
T4	1 (0.6)
Pathological Gleason grade group, *n* (%)	
ISUP 1	4 (2.2)
ISUP 2	63 (35.4)
ISUP 3	57 (32.0)
ISUP 4	3 (1.7)
ISUP 5	51 (28.7)
Surgical margin, *n* (%)	
Positive	56 (31.5)
Negative	122 (68.5)

IQR, interquartile range; PSA, prostate-specific antigen; ISUP, International Society of Urological Pathology.

Overall, the side-specific models presented higher AUC than the non-side-specific models (Table 3). Among the formers, the Soeterik nomogram presented excellent discrimination with the higher AUC, followed by the Patel, Sayyid, Martini, and Steuber models. However, the 95% confidence interval for most of these models overlapped. Among the latter, the MSKCC web calculator with and without the total number of cores involvement presented the higher AUC, followed by the Roach formula, and Partin tables. Receiver operating characteristic plots showing the AUC are shown in Fig. 1. The new versions of Partin tables performed slightly better than the previous versions. The MSKCC web calculators with or without biopsy cores performed similarly. Calibration plots for side-specific models are shown in Fig. 2. The Soeterik model had the better calibration performance. However, this model overestimated the risk of ECE in low and high ranges (predicted risk of <10% and predicted risk >80%), and slightly underestimated the risk of ECE in media ranges. The Patel and Martini models calibrated similarly, and both underestimated in low- and high-risk ranges. The Sayyid and Steuber models underestimated in low ranges and overestimated in medium ranges. Regarding the non-side-specific models, all of them presented a poor calibration performance (Supplementary Fig. 1).

Table 2 Baseline characteristics with comparison between groups with positive and negative extracapsular extension.

Variable	All lobes ($n=356$)	ECE positive ($n=117$)	ECE negative ($n=239$)	p-Value
Age, *n* (%)				0.051
<50 years	12 (3.4)	3 (2.6)	9 (3.8)	
50–59 years	60 (16.9)	16 (13.7)	44 (18.4)	
60–69 years	218 (61.2)	67 (57.3)	151 (63.2)	
≥70 years	66 (18.5)	31 (26.5)	35 (14.6)	
Median PSA, *n* (%)				<0.001
<10 ng/mL	230 (64.6)	56 (47.9)	174 (72.8)	
10–20 ng/mL	88 (24.7)	36 (30.8)	52 (21.8)	
>20 ng/mL	38 (10.7)	25 (21.4)	13 (5.4)	
Digital rectal examination, *n* (%)				<0.001
Positive	107 (30.1)	54 (46.2)	53 (22.2)	
Negative	249 (69.9)	63 (53.8)	186 (77.8)	
Hypoechoic nodule in TRUS, *n* (%)				<0.001
Present	87 (24.4)	46 (39.3)	41 (17.2)	
Absent	269 (75.6)	71 (60.7)	198 (82.8)	
Magnetic resonance imaging nodes, *n* (%)				<0.001
ECE positive	29 (8.1)	23 (19.7)	6 (2.5)	
ECE negative	100 (28.1)	55 (47.0)	45 (18.8)	
No nodule	227 (63.8)	39 (33.3)	188 (78.7)	
Ipsilateral Gleason grade group, *n* (%)				<0.001
No cancer	81 (22.8)	7 (6.0)	74 (31.0)	
ISUP 1	77 (21.6)	12 (10.3)	65 (27.2)	
ISUP 2	73 (20.5)	32 (27.4)	41 (17.2)	
ISUP 3	67 (18.8)	31 (26.5)	36 (15.1)	
ISUP 4	37 (10.4)	21 (17.9)	16 (6.7)	
ISUP 5	21 (5.9)	14 (12.0)	7 (2.9)	
Positive core ratio, *n* (%)				<0.001
0–25%	185 (52.0)	40 (34.2)	145 (60.7)	
26%–50%	95 (26.7)	28 (23.9)	67 (28.0)	
51%–75%	32 (9.0)	16 (13.7)	16 (6.7)	
76%–100%	44 (12.4)	33 (28.2)	11 (4.6)	
Maximum core involvement ratio, *n* (%)				<0.001
0–25%	205 (57.6)	40 (34.2)	165 (69.0)	
26%–50%	71 (19.9)	30 (25.6)	41 (17.2)	
51%–75%	22 (6.2)	8 (6.8)	14 (5.9)	
76%–100%	58 (16.3)	39 (33.3)	19 (7.9)	

ECE, extracapsular extension; TRUS, transrectal ultrasound; PSA, prostate-specific antigen; ISUP, International Society of Urological Pathology.

Note: total percentages may not be 100% due to rounding.

In the decision curve analyses, all side-specific models showed net benefit, but they overlapped among them (Fig. 3). The non-side-specific models presented net benefit, except for the Partin tables (Supplementary Fig. 2).

4. Discussion

Among the side-specific models, the Soeterik model presented excellent discrimination with the higher AUC (0.81) followed by the Patel model AUC (0.78), the Sayyid nomogram AUC (0.77), the Martini nomogram AUC (0.75), and the Steuber model AUC (0.73). On the other hand, among the non-side-specific models, the MSKCC web calculator presented higher AUC (0.74), followed by Roach formula AUC (0.72), and the Partin tables of 2016 AUC (0.64), 2013 AUC (0.61), and 2007 AUC (0.60). Thus, the side-specific models presented higher AUCs than the non-side-specific ones. The 95% confidence interval for most of these models overlapped. However, the Soeterik model also presented the best calibration performance.

There is heterogeneity in the variables included in the side-specific models. All of them include PSA level, except the Soeterik model that includes PSA density. Soeterik and Martini nomograms include MRI findings, and Sayyid nomogram includes transrectal ultrasound findings. The Patel model includes the biopsy core involvement and the ISUP grade group for each core, while the others include the greater percentage of core involvement. Another difference is that the Sayyid and Martini nomograms do not predict a probability of ECE in a lobe without tumor, contrary to Soeterik, Steuber, and Patel nomograms. These models consider that, despite not having carcinoma in biopsy cores, the probability to have ECE is higher than

Table 3 Results for the validated models and their updates.

Predictive model	Parameters utilized in model	AUC (95% CI)
Side-specific model		
Soeterik	- PSA density, MRI clinical, total Gleason score	0.81 (0.76—0.86)
Steuber	- PSA, clinical T-stage, total Gleason score, percentage of positive BCs, percentage of cancer in biopsy specimen	0.73 (0.68—0.78)
Sayyid	- Age, PSA, clinical T-stage, total Gleason score, maximum percentage of core involvement, percentage of positive BCs, hypoechoic nodule	0.77 (0.71—0.82)
Martini	- PSA, total Gleason score, maximum percentage of core involvement, ECE in MRI	0.75 (0.70—0.81)
Patel	- Age, PSA, total Gleason score in positive core, clinical T-stage, percentage of in tumor positive	0.78 (0.73—0.83)
Non-side-specific model		
Roach formula	- PSA, total Gleason score	0.72 (0.64—0.79)
Partin tables		
Makarov	- PSA, clinical T-stage, total Gleason score	0.60 (0.51—0.68)
Eifel	- PSA, clinical T-stage, total Gleason score	0.61 (0.53—0.70)
Tosoian	- PSA, clinical T-stage, total Gleason score	0.64 (0.56—0.73)
MSKCC		
Web calculator (incl. BCs)	- Age, PSA, clinical T-stage, primary and secondary Gleason, percentage of BCs	0.74 (0.67—0.81)
Web calculator (excl. BCs)	- Age, PSA, clinical T-stage, primary and secondary Gleason	0.74 (0.67—0.81)

AUC, area under the curve; BCs, biopsy cores; ECE, extracapsular extension; excl., excluding; incl., including; MRI, magnetic resonance imaging; CI, confidence interval; MSKCC, Memorial Sloan Kettering Cancer Center; PSA, prostate-specific antigen.

zero in lobes with contralateral higher ISUP grade group, percentage of cancer involvement, or PSA. In fact, in the present study, ECE was positive in 8.8% (7/80) of prostate lobes without tumor in the biopsy. The Patel model predicts the overall risk of ECE, and at 1, 2, 3, and 4 mm. However, we only validated the presence or not of ECE to compare with the other models included. On the other hand, the non-side-specific models are more homogeneous in the variables included and most of them included PSA, clinical T-stage, and ISUP grade group.

Rocco et al. [30] performed an external validation of several models predicting ECE using the data of 6360 prostate cancer patients undergoing radical prostatectomy. They found that most of the Partin tables were not reliable and showed poor discrimination and unsatisfactory calibration. Additionally, the Steuber nomogram presented acceptable discrimination, but lower than that in the development population, and unsatisfactory calibration. However, most of these patients were from the USA, and the models included did not have MRI among variables. Another study suggested that the validated models are not reliable in the context of high-risk prostate cancer [31].

Supplementary Table 1 shows an overview of previous validation studies. The Partin tables published in 2001 were validated in a Japanese cohort in 2008 [25]. However, several other updates to these tables were subsequently performed [19—21]. To the best of our knowledge, this is the first external validation of the MSKCC web calculator with or without the total number of cores involvement, the Patel model, Sayyid model, and Soeterik model. Moreover, this study is also the first validation of new versions of the Partin tables and the Steuber models in Japanese.

Meanwhile, we found that AUCs in this study ranged among AUCs found in previous validations conducted mainly in European and North American countries (Supplementary Table 1). When comparing to other validation studies, our AUCs differed because of several factors: different biopsy approaches (transrectal or transperitoneal), biopsy techniques with the inclusion or exclusion of MRI, and the number of cores taken in each case; the decision to perform NSRP; and the characteristics of the population included. The proportion of prostate lobes with ECE included in the models ranged between 7% and 32% [15,32]. Moreover, there were differences in the clinicopathological characteristics among included patients. In addition, some studies included a larger number of databases, surgeons, or pathologists. Moreover, some studies mixed different surgical approaches (open, laparoscopic, or RARP). This is a single-center study, and RARP was performed in all patients and included a few surgeons and pathologists. Finally, ethnic differences could explain differences in prostate cancer behavior [33,34].

In the calibration plots, the Soeterik, Partin, Martini, and Sayyid models presented adequate calibration and presented the lowest prediction variability. However, the four of them overestimated the risk of ECE in patients with predicted ECE lower than 10%. Thus, in these patients, the observed risk of ECE may be 10%—20% lower. Current urology guidelines do not set a limit to recommend against performing NSRP. Setting a limit in 20% and 25%, using the Soeterik model in this cohort, NSRP would have been incorrectly omitted in 7.5% and 9.8% of patients, respectively. Using the same cut-off values using the Patel model resulted in 14.3% and 10.7% of false negatives.

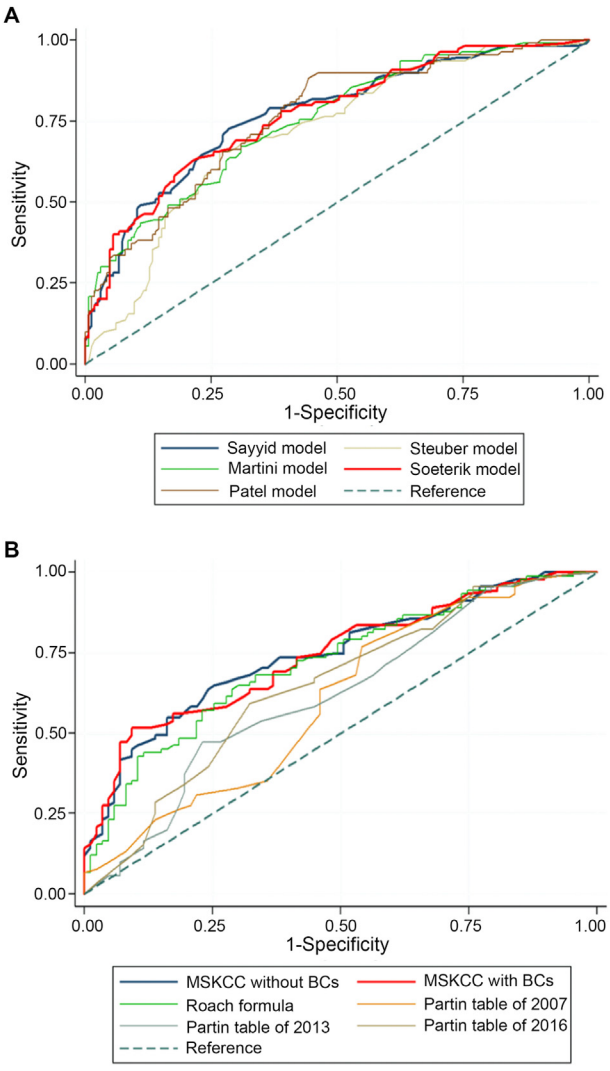

Figure 1 Receiving operator characteristic curves. (A) The side-specific models; (B) The non-side-specific models. MSKCC, Memorial Sloan Kettering Cancer Center; BCs, biopsy cores.

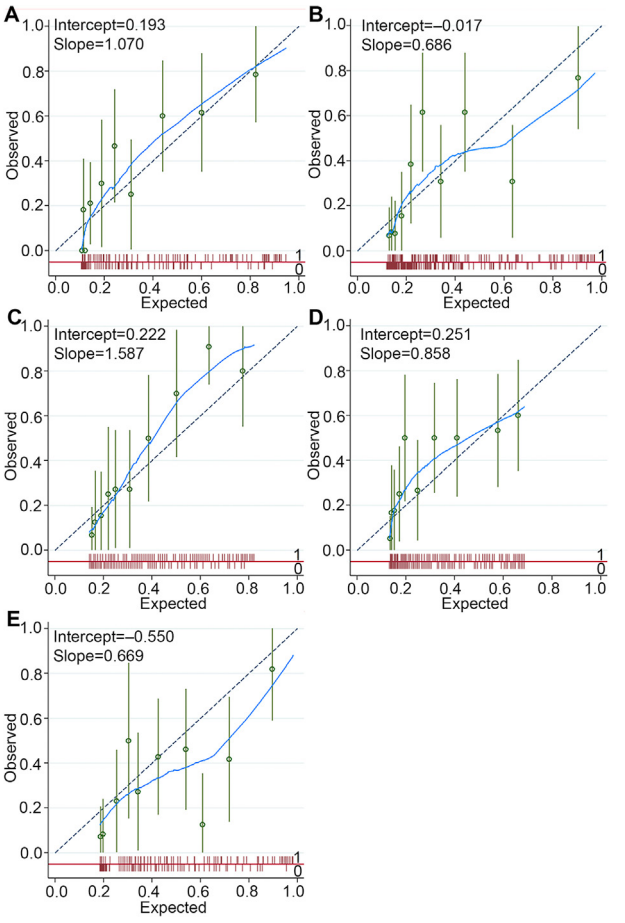

Figure 2 Calibration plots for the models. (A) The Soeterik model; (B) The Patel model; (C) The Sayyid model; (D) The Steuber model; (E) The Martini model. The expected risk is divided into ten equally sized groups. The green dots and spikes are media risks and 95% confidence intervals. The dotted line is the reference line of calibration. The blue line is obtained by locally weighted scatterplot smoothing. The red spike plot gives the distribution of extracapsular extension (0=no; 1=yes).

Several papers have shown that the extent of ECE is associated with a poor prognosis [35,36]. However, there is no consensus on how to evaluate the extent of ECE. The Epstein criteria define focal extension as a few neoplastic glands beyond the limits of the prostate on no more than two separate sections, and non-focal extension as more than focal [35]. Meanwhile, other authors used the radial distance to measure the extent of ECE [36]. Recently, two studies with a large population using the Epstein criteria showed that both non-focal ECE and focal ECE were independently associated with a worse prognosis than patients without ECE. Non-focal and focal ECE were independent risk factors for biochemical recurrence [37,38]. Ten-year cancer-specific survival and overall survival in patients with isolated ECE were not significantly different between patients with focal or non-focal ECE [38].

Recently, the inclusion of artificial intelligence in MRI models compared to experts presented promising results [39]. Moreover, there is still an unknown role for genetic in this field such as *PTEN* and endothelin-1. The development

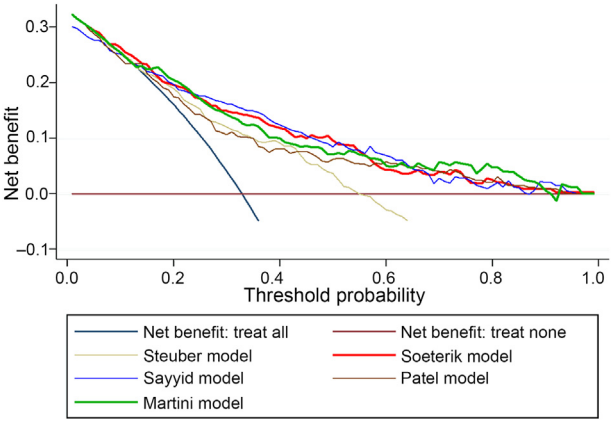

Figure 3 Decision curve analyses of the Soeterik, the Patel, the Sayyid, the Steuber, and the Martini models.

of nomograms that include artificial intelligence and genetic could be a future perspective to predict ECE and improve surgical management.

5. Conclusion

Among all evaluated models, the side-specific models showed acceptable to excellent performance with an AUC of 0.73—0.81 and predicted better than the non-side-specific models. The side-specific models presented adequate calibration, net benefit, and had the lowest prediction variability. The best-performing nomograms were the Soeterik and the Patel models. Then, these models can be utilized for the prediction of ECE in Japanese who undergo NSRP.

Author contributions

Study concept and design: Leandro Blas, Masaki Shiota.
Data acquisition: Leandro Blas, Masaki Shiota, Shohei Nagakawa, Shigehiro Tsukahara, Takashi Matsumoto, Ken Lee, Keisuke Monji, Eiji Kashiwagi, Junichi Inokuchi, Masatoshi Eto.
Data analysis: Leandro Blas, Masaki Shiota.
Drafting of manuscript: Leandro Blas, Masaki Shiota.
Critical revision of the manuscript: Leandro Blas, Masaki Shiota.

Conflicts of interest

The authors declare no conflict of interest.

Appendix A. Supplementary data

Supplementary data to this article can be found online at https://doi.org/10.1016/j.ajur.2022.02.008.

References

[1] Patel VR, Sivaraman A, Coelho RF, Chauhan S, Palmer KJ, Orvieto MA, et al. Pentafecta: a new concept for reporting outcomes of robot-assisted laparoscopic radical prostatectomy. Eur Urol 2011;59:702—7.

[2] Reeves F, Preece P, Kapoor J, Everaerts W, Murphy DG, Corcoran NM, et al. Preservation of the neurovascular bundles is associated with improved time to continence after radical prostatectomy but not long-term continence rates: results of a systematic review and meta-analysis. Eur Urol 2015;68:692—704.

[3] Druskin SC, Liu JJ, Young A, Feng Z, Dianat SS, Ludwig WW, et al. Prostate MRI prior to radical prostatectomy: effects on nerve sparing and pathological margin status. Res Rep Urol 2017;9:55—63.

[4] Martini A, Marqueen KE, Falagario UG, Waingankar N, Wajswol E, Khan F, et al. Estimated costs associated with radiation therapy for positive surgical margins during radical prostatectomy. JAMA Netw Open 2020;3:e201913. https://doi.org/10.1001/jamanetworkopen.2020.1913.

[5] Magi-Galluzzi C, Evans AJ, Delahunt B, Epstein JI, Griffiths DF, van der Kwast TH, et al. International Society of Urological Pathology (ISUP) consensus conference on handling and staging of radical prostatectomy specimens. Working group 3: extraprostatic extension, lymphovascular invasion and locally advanced disease. Mod Pathol 2011;24:26—38.

[6] Amling CL, Blute ML, Lerner SE, Bergstralh EJ, Bostwick DG, Zincke H. Influence of prostate-specific antigen testing on the spectrum of patients with prostate cancer undergoing radical prostatectomy at a large referral practice. Mayo Clin Proc 1998;73:401—6.

[7] Mottet N, van den Bergh RCN, Briers E, Van den Broeck T, Cumberbatch MG, De Santis M, et al. EAU-EANM-ESTRO-ESUR-SIOG guidelines on prostate cancer—2020 update. Part 1: screening, diagnosis, and local treatment with curative intent. Eur Urol 2021;79:243—62.

[8] Somford DM, Hamoen EH, Fütterer JJ, van Basten JP, Hulsbergen-van de Kaa CA, Vreuls W, et al. The predictive value of endorectal 3 Tesla multiparametric magnetic resonance imaging for extraprostatic extension in patients with low, intermediate and high risk prostate cancer. J Urol 2013;190:1728—34.

[9] Mohler JL, Antonarakis ES, Armstrong AJ, D'Amico AV, Davis BJ, Dorff T, et al. Prostate cancer, version 2.2019, NCCN clinical practice guidelines in oncology. J Natl Compr Cancer Netw 2019;17:479—505.

[10] de Rooij M, Hamoen EHJ, Witjes JA, Barentsz JO, Rovers MM. Accuracy of magnetic resonance imaging for local staging of prostate cancer: a diagnostic meta-analysis. Eur Urol 2016;70:233—45.

[11] Gandaglia G, De Lorenzis E, Novara G, Fossati N, De Groote R, Dovey Z, et al. Robot-assisted radical prostatectomy and extended pelvic lymph node dissection in patients with locally-advanced prostate cancer. Eur Urol 2017;71:249—56.

[12] Yuh B, Artibani W, Heidenreich A, Kimm S, Menon M, Novara G, et al. The role of robot-assisted radical prostatectomy and pelvic lymph node dissection in the management of high-risk prostate cancer: a systematic review. Eur Urol 2014;65:918—27.

[13] Sayyid R, Perlis N, Ahmad A, Evans A, Toi A, Horrigan M, et al. Development and external validation of a biopsy-derived nomogram to predict risk of ipsilateral extraprostatic extension. BJU Int 2017;120:76—82.

[14] Martini A, Gupta A, Lewis SC, Cumarasamy S, Haines 3rd KG, Briganti A, et al. Development and internal validation of a side-specific, multiparametric magnetic resonance imaging-based nomogram for the prediction of extracapsular extension of prostate cancer. BJU Int 2018;122:1025—33.

[15] Patel VR, Sandri M, Grasso AAC, De Lorenzis E, Palmisano F, Albo G, et al. A novel tool for predicting extracapsular extension during graded partial nerve sparing in radical prostatectomy. BJU Int 2018;121:373—82.

[16] Steuber T, Graefen M, Haese A, Erbersdobler A, Chun FK, Schlom T, et al. Validation of a nomogram for prediction of side specific extracapsular extension at radical prostatectomy. J Urol 2006;175:939—44.

[17] Soeterik TFW, van Melick HHE, Dijksman LM, Küsters-Vandevelde H, Stomps S, Schoots IG, et al. Development and external validation of a novel nomogram to predict side-specific extraprostatic extension in patients with prostate cancer undergoing radical prostatectomy. Eur Urol Oncol 2020;S2588—9311:30133—4. https://doi.org/10.1016/j.euo.2020.08.008.

[18] Memorial Sloan Kettering Cancer Center. Pre-radical prostatectomy tool to predict probability of lymph node involvement in prostate cancer patients. www.mskcc.org/nomograms/prostate/pre_op. [Accessed 6 June 2021].

[19] Makarov DV, Trock BJ, Humphreys EB, Mangold LA, Walsh PC, Epstein JI, et al. Updated nomogram to predict pathologic stage of prostate cancer given prostate-specific antigen level,

clinical stage, and biopsy Gleason score (Partin tables) based on cases from 2000 to 2005. Urology 2007;69:1095—101.
[20] Eifler JB, Feng Z, Lin BM, Partin MT, Humphreys EB, Han M, et al. An updated prostate cancer staging nomogram (Partin tables) based on cases from 2006 to 2011. BJU Int 2013;111: 22—9.
[21] Tosoian JJ, Chappidi M, Feng Z, Humphreys EB, Han M, Pavlovich CP, et al. Prediction of pathological stage based on clinical stage, serum prostate-specific antigen, and biopsy Gleason score: Partin tables in the contemporary era. BJU Int 2017;119:676—83.
[22] Sanda MG, Cadeddu JA, Kirkby E, Chen RC, Crispino T, Fontanarosa J, et al. Clinically localized prostate cancer: AUA/ASTRO/SUO guideline. Part II: recommended approaches and details of specific care options. J Urol 2018; 199:990—7.
[23] Kakehi Y, Sugimoto M, Taoka R. Evidenced-based clinical practice guideline for prostate cancer (summary: Japanese Urological Association, 2016 edition). Int J Urol 2017;24:648—66.
[24] Murakami T, Otsubo S, Namitome R, Shiota M, Inokuchi J, Takeuchi A, et al. Clinical factors affecting perioperative outcomes in robot-assisted radical prostatectomy. Mol Clin Oncol 2018;9:575—81.
[25] Naito S, Kuroiwa K, Kinukawa N, Goto K, Koga H, Ogawa O, et al. Validation of Partin tables and development of a preoperative nomogram for Japanese patients with clinically localized prostate cancer using 2005 International Society of Urological Pathology consensus on Gleason grading: data from the clinicopathological. J Urol 2008;180:904—10.
[26] D'Amico AV, Whittington R, Bruce Malkowicz S, Schultz D, Blank K, Broderick GA, et al. Biochemical outcome after radical prostatectomy, external beam radiation therapy, or interstitial radiation therapy for clinically localized prostate cancer. J Am Med Assoc 1998;280:969—74.
[27] Roach M, Marquez C, Yuo HS, Narayan P, Coleman L, Nseyo UO, et al. Predicting the risk of lymph node involvement using the pre-treatment prostate specific antigen and Gleason score in men with clinically localized prostate cancer. Int J Radiat Oncol Biol Phys 1994;28:33—7.
[28] Hosmer JDW, Lemeshow S, Sturdivant RX. Applied logistic regression. 3rd ed. Hoboken, NJ, USA: John Wiley & Sons; 2013. p. 177.
[29] Vickers AJ, van Calster B, Steyerberg EW. A simple, step-by-step guide to interpreting decision curve analysis. Diagnostic Progn Res 2019;3:1—8.
[30] Rocco B, Sighinolfi MC, Sandri M, Eissa A, Elsherbiny A, Zoeir A, et al. Is extraprostatic extension of cancer predictable? A review of predictive tools and an external validation based on a large and a single center cohort of prostate cancer patients. Urology 2019;129:8—20.
[31] Martini A, Soeterik TFW, Haverdings H, Rahota RG, Checcucci E, De Cillis S, et al. An algorithm to personalize nerve sparing in men with unilateral high-risk prostate cancer. J Urol 2022;207:350—7.
[32] Soeterik TFW, van Melick HHE, Dijksman LM, Küsters-Vandevelde HVN, Biesma DH, Witjes JA, et al. External validation of the Martini nomogram for prediction of side-specific extraprostatic extension of prostate cancer in patients undergoing robot-assisted radical prostatectomy. Urol Oncol Semin Orig Investig 2020;38:372—8.
[33] Song C, Ro JY, Lee MS, Hong SJ, Chung BH, Choi HY, et al. Prostate cancer in Korean men exhibits poor differentiation and is adversely related to prognosis after radical prostatectomy. Urology 2006;68:820—4.
[34] Byun SS, Lee S, Lee SE, Lee E, Seo SI, Lee HM, et al. Recent changes in the clinicopathologic features of Korean men with prostate cancer: a comparison with Western populations. Yonsei Med J 2012;53:543—9.
[35] Epstein JI, Carmichael MJ, Pizov G, Walsh PC. Influence of capsular penetration on progression following radical prostatectomy: a study of 196 cases with long-term followup. J Urol 1993;150:135—41.
[36] Sung MT, Lin H, Koch MO, Davidson DD, Cheng L. Radial distance of extraprostatic extension measured by ocular micrometer is an independent predictor of prostate-specific antigen recurrence: a new proposal for the substaging of pT3a prostate cancer. Am J Surg Pathol 2007;31:311—8.
[37] Ball MW, Partin AW, Epstein JI. Extent of extraprostatic extension independently influences biochemical recurrence-free survival: evidence for further PT3 subclassification. Urology 2015;85:161—4.
[38] Jeong BC, Chalfin HJ, Lee SB, Feng Z, Epstein JI, Trock BJ, et al. The relationship between the extent of extraprostatic extension and survival following radical prostatectomy. Eur Urol 2015;67:342—6.
[39] Hou Y, Zhang YH, Bao J, Bao ML, Yang G, Shi HB, et al. Artificial intelligence is a promising prospect for the detection of prostate cancer extracapsular extension with mpMRI: a two-center comparative study. Eur J Nucl Med Mol Imaging 2021; 48:3805—16.